European Journal of Radiology 144 (2021) 109958

Contents lists available at ScienceDirect

European Journal of Radiology

journal homepage: www.elsevier.com/locate/ejrad

Noninvasive assessment of clinically significant portal hypertension using ΔT1 of the liver and spleen and ECV of the spleen on routine Gd-EOB-DTPA liver MRI

Damiano Catucci [a], Verena Carola Obmann [a], Annalisa Berzigotti [b], Christoph Gräni [c], Dominik Paul Guensch [a,d], Kady Fischer [d], Lukas Ebner [a], Johannes Thomas Heverhagen [a], Andreas Christe [a], Adrian Thomas Huber [a,*]

[a] Department of Diagnostic, Interventional and Pediatric Radiology, Inselspital, Bern University Hospital, University of Bern, Switzerland
[b] Hepatology, Department of Visceral Surgery and Medicine, Inselspital, Bern University Hospital, University of Bern, Switzerland
[c] Department of Cardiology, Inselspital, Bern University Hospital, University of Bern, Switzerland
[d] Department of Anaesthesiology and Pain Medicine, Inselspital, Bern University Hospital, University of Bern, Bern, Switzerland

ARTICLE INFO

Keywords:
Liver diseases
Portal hypertension
Magnetic resonance imaging
Venous congestion
Splenomegaly
T1 mapping

ABSTRACT

Purpose: To analyze the predictive value of ΔT1 of the liver and spleen as well as the extracellular volume fraction (ECV) of the spleen as noninvasive biomarkers for the determination of clinically significant portal hypertension (CSPH) on routine Gd-EOB-DTPA liver MRI.

Method: 195 consecutive patients with known or suspected chronic liver disease from 9/2018 to 7/2019 with Gd-EOB-DTPA liver MRI and abdominal T1 mapping were retrospectively included. Based on the presence of splenomegaly with thrombocytopenia, ascites and portosystemic collaterals, the patients were divided into noCSPH (n = 113), compensated CSPH (cCSPH, ≥1 finding without ascites; n = 55) and decompensated CSPH (dCSPH, ascites ± other findings; n = 27). T1 times were measured in the liver, spleen and abdominal aorta in the unenhanced and contrast-enhanced T1 maps. Native T1 times and ΔT1 of the liver and spleen as well as ECV of the spleen were compared between groups using the Kruskal-Wallis test with Dunn's post hoc test. Furthermore, cutoff values for group differentiation were calculated using ROC analysis with Youden's index.

Results: ΔT1 of the liver was significantly lower in patients with cCSPH and dCSPH ($p < 0.001$) compared to patients with noCSPH. In the ROC analyses for differentiation between noCSPH and CSPH (cCSPH + dCSPH), a cutoff of < 0.67 for ΔT1 of the liver (AUC = 0.79) performed better than ΔT1 (AUC = 0.69) and ECV (AUC = 0.63) of the spleen with cutoffs of > 0.29 and > 41.9, respectively.

Conclusion: ΔT1 of the liver and spleen in addition to ECV of the spleen allow for determination of CSPH on routine Gd-EOB-DTPA liver MRI.

Abbreviations and acronyms: **ALT**, Alanine aminotransferase; **AP**, Alkaline phosphatase; **APRI**, Aminotransferase to platelet ratio index; **ARLD**, Alcohol-related liver disease; **ASH**, Alcoholic steatohepatitis; **AST**, Aspartate aminotransferase; **AUROC**, Area under the receiver operating characteristic curve; **BMI**, Body mass index; **cCSPH**, Compensated clinically significant portal hypertension; **CLD**, Chronic liver disease; **CSPH**, Clinically significant portal hypertension; **dCSPH**, Decompensated clinically significant portal hypertension; **DWI**, Diffusion-weighted imaging; **ECV**, Extracellular volume fraction; **FIB-4**, Fibrosis-4 index; **FS**, Fat-saturated; **Gd-EOB-DTPA**, Gadolinium ethoxybenzyl diethylenetriamine pentaacetic acid; **GGT**, Gamma-glutamyl transpeptidase; **HASTE**, Half-Fourier acquisition single-shot turbo spin echo; **HVPG**, Hepatic venous pressure gradient; **LSN**, Liver surface nodularity; **MIP**, Maximum intensity projection; **MRE**, Magnetic resonance elastography; **NAFLD**, Nonalcoholic fatty liver disease; **NASH**, Nonalcoholic steatohepatitis; **NPV**, Negative predictive value; **OATP**, Organic anion transporting polypeptide; **PBC**, Primary biliary cholangitis; **PPV**, Positive predictive value; **PSC**, Primary sclerosing cholangitis; **shMOLLI**, Shortened modified look-locker inversion recovery; **TIPS**, Trans-jugular intrahepatic portosystemic shunt; **VIBE**, Volumetric interpolated breath-hold examination.

* Corresponding author at: Department of Diagnostic, Interventional and Pediatric Radiology, Freiburgstrasse 10, Inselspital, 3010 Bern, Switzerland.
E-mail addresses: damiano.catucci@extern.insel.ch (D. Catucci), verena.obmann@insel.ch (V.C. Obmann), annalisa.berzigotti@insel.ch (A. Berzigotti), christoph.graeni@insel.ch (C. Gräni), dominik.guensch@insel.ch (D.P. Guensch), kady.fischer@insel.ch (K. Fischer), lukas.ebner@insel.ch (L. Ebner), johannes.heverhagen@insel.ch (J.T. Heverhagen), andreas.christe@insel.ch (A. Christe), adrian.huber@insel.ch (A.T. Huber).

https://doi.org/10.1016/j.ejrad.2021.109958
Received 28 April 2021; Received in revised form 23 August 2021; Accepted 15 September 2021
Available online 20 September 2021

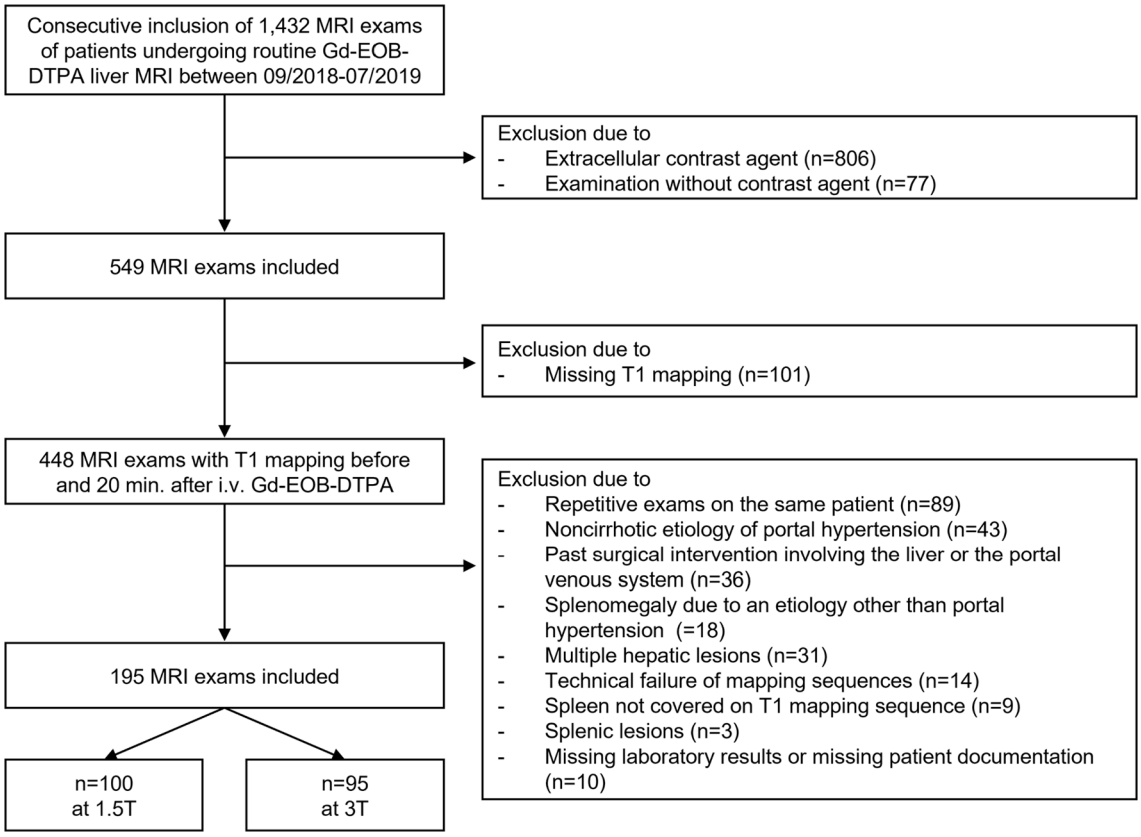

Fig. 1. Flowchart of the study population.

1. Introduction

Patients with chronic liver disease (CLD) and, in particular, cirrhosis have a high risk of developing clinically significant portal hypertension (CSPH) [1,2]. CSPH is associated with potentially fatal complications, such as variceal hemorrhage, ascites, hepatic encephalopathy, renal dysfunction, and adverse outcomes after liver surgery and transarterial chemoembolization [2–6]. Currently, liver cirrhosis is the fourth leading cause of death in the adult population of Central Europe and is responsible for approximately 170,000 deaths annually in Europe, and the majority of deaths are not due to hepatocyte failure but instead are due to complications associated with CSPH [7,8]. Noninvasive imaging biomarkers may allow for determining the presence or absence of CSPH for a better characterization of CLD and outcome prediction before planned liver surgery or endovascular interventions [2,9].

Magnetic resonance (MR) biomarkers to determine the presence of CSPH are mainly focused on liver segmental volumes, segmental volume ratios [10] and spleen size [11] as well as the presence or absence of liver surface nodularity [12], ascites and portosystemic collaterals [13]. T1 mapping techniques have shown promising results to quantify liver fibrosis and to determine the degree of liver inflammation in CLD [14,15]. Another method that has already been studied in the context of CSPH is MR elastography (MRE). MRE allows a noninvasive quantitative measurement of the hepatic and splenic stiffness [16], which may represent a helpful biomarker for the characterization of patients with CSPH, as an increased splenic stiffness is associated with CSPH and gastroesophageal varices [17,18]. Recently, the T1 mapping-derived extracellular volume fraction (ECV) of the spleen has been shown to be able to distinguish between healthy volunteers and patients with severe portal hypertension undergoing a transjugular intrahepatic portosystemic shunt (TIPS) procedure [6]. This proof-of-concept study has demonstrated that MR T1 mapping techniques have good potential, not only when measured in the liver but also in the spleen. However, the abovementioned study is limited by the differentiation between healthy volunteers and a small group of patients with end-stage liver cirrhosis and severe portal hypertension, in which the differences are obvious. Validation in a clinical setting with more heterogeneous patients undergoing liver MRI is therefore needed.

Another possible limitation for the use of ECV in routine clinical liver MRI is that ECV calculation is based on the use of MR contrast agents with extracellular distribution, while routine clinical liver MRI is often performed using hepatocyte-specific contrast agents, such as gadolinium ethoxybenzyl diethylenetriamine pentaacetic acid (Gd-EOB-DTPA). Instead of distributing to the extracellular space as an extracellular contrast agent, approximately 50% of circulating Gd-EOB-DTPA is actively taken up from hepatic sinusoids into hepatocytes by organic anion-transporting polypeptides (OATP1B1 and OATP1B3) [19,20], thereby rendering ECV calculation in the liver impossible. Because Gd-EOB-DTPA is a paramagnetic substance that shortens the longitudinal relaxation (T1) time, ΔT1 of the liver can be calculated as a noninvasive imaging biomarker to quantify hepatocellular function. ΔT1 represents the difference in the T1 relaxation time before and after Gd-EOB-DTPA application in the hepatobiliary phase [19].

Because the spleen has no hepatocytes, the remaining 50% of Gd-EOB-DTPA without hepatobiliary clearance may act similarly to an extracellular agent in the spleen, thereby allowing the calculation of the ECV in the spleen. Additionally, calculation of ΔT1 in the spleen may be a simplified but robust alternative to the complex ECV evaluation without the need to know the patient's hematocrit as previously shown in myocardial and skeletal muscles [21]. Both the ECV and ΔT1 may be calculated in the spleen to determine the extent of splenic extracellular space using a Gd-EOB-DTPA liver MRI. It has not been previously reported whether ΔT1 of the liver along with ΔT1 and ECV of the spleen allow the determination of CSPH using routine clinical Gd-EOB-DTPA MRI.

The present study analyzed the predictive value of ΔT1 of the liver

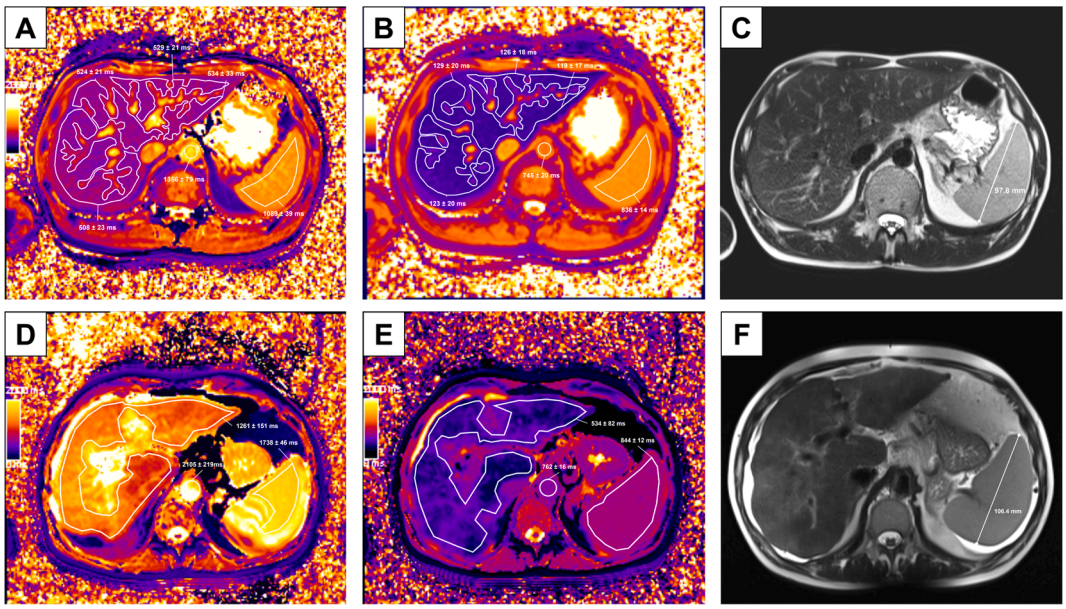

Fig. 2. Measurements of T1 relaxation time and spleen size. Fig. 2. In images A to C, the assessment of a 36-year-old male patient without chronic liver disease and no clinically significant portal hypertension (noCSPH) is shown. In images D to F, the same assessment is shown for a 60-year-old female patient with alcoholic liver cirrhosis (Child B) and decompensated clinically significant portal hypertension (dCSPH). In A and D, ROIs are placed in the liver, abdominal aorta and spleen on the native T1 map. In B and E, ROIs are placed in the liver, abdominal aorta and spleen on the T1 map 20 min after the administration of Gd-EOB-DTPA. In C and F, measurement of the spleen is shown on a T2-weighted half-Fourier acquisition single-shot turbo spin echo (HASTE) sequence. For the 36-year-old patient with noCSPH, we calculated a ΔT1 of the liver of 0.75, a ΔT1 of the spleen of 0.23 and an ECV of the spleen of 30.8. For the 60-year-old patient with dCSPH, we calculated a ΔT1 of the liver of 0.59, a ΔT1 of the spleen of 0.53 and an ECV of the spleen of 48.2.

and spleen and the extracellular volume fraction of the spleen as noninvasive biomarkers for the determination of clinically significant portal hypertension (CSPH) using routine Gd-EOB-DTPA liver MRI.

2. Material and methods

2.1. Study population

The Institutional Review Board approved this retrospective study. All patients gave written informed consent or were informed without dissent. We screened 1,432 consecutive abdominal MR examinations from our hospital database between September 2018 and July 2019. Exams using extracellular contrast agents (n = 806) or no contrast agent (n = 77) were excluded. From the resulting 549 dedicated liver MRIs with Gd-EOB-DTPA, 101 were excluded due to missing T1 mapping. Other MRI exams were excluded for the following reasons: repetitive exams on the same patient (n = 89, only the first exam of each patient was included); noncirrhotic etiology of portal hypertension (n = 43); past surgical intervention involving the liver or the portal venous system (n = 36); splenomegaly due to an etiology other than portal hypertension (n = 18); patients with multiple hepatic lesions (n = 31); technical failure of T1 mapping sequences (n = 14); spleen not covered on T1 mapping sequence (n = 9); and splenic lesions (n = 3). Finally, 10 patients were excluded due to missing laboratory results or missing patient documentation. Thus, the final study population included 195 patients, from which 100 patients were examined at 1.5T and 95 patients were examined at 3T (Fig. 1).

2.2. Imaging techniques

All MRI examinations were performed using a whole-body 1.5 Tesla MR system (Magnetom Aera 1.5T, Siemens Healthineers, Erlangen, Germany, n = 100) or a whole-body 3 Tesla MR system (Magnetom Skyra 3T, Siemens Healthineers, Erlangen, Germany, n = 95). The imaging protocols were the same at 1.5T and 3T. The standard Gd-EOB-DTPA liver protocol was as follows: a T1 volumetric interpolated breath-hold examination (VIBE) DIXON 3 mm transversal acquisition of the liver, a half-Fourier single-shot turbo spin-echo (HASTE) sequence 3 mm transversal and coronal acquisition of the liver; a diffusion-weighted imaging (DWI) sequence with b = 0, b = 400 and b = 800 s/mm^2 values; and T1 VIBE fat-saturated (fs) transversal 3 mm acquisitions before and after intravenous contrast administration in arterial, venous, delayed and hepatobiliary phases after 10 and 20 min. Apart from the standard Gd-EOB-DTPA liver imaging protocol, native axial T1 mapping sequences and axial T1 mapping sequences 20 min after intravenous administration of 0.25 mmol Gd-EOB-DTPA (Primovist®, Bayer Healthcare, Berlin, Germany) per kilogram body weight were performed. Specifications of the sequences used are listed in Table A in the appendix. For T1 mapping, shortened modified look-locker inversion recovery (shMOLLI) single breath-hold sequences with a 5(1)1(1)1 protocol were used, and images were acquired during a breath-hold time of 7–9 s at end-expiration. The total scan time per T1 mapping sequence was less than 2 min before and after the application of the contrast agent, resulting in a total additional scan time of less than 4 min per patient. The scan duration was the same on 1.5T and 3T. To our knowledge, this MR T1 mapping protocol has previously been used to determine ΔT1 of the liver but not in the spleen [20]. The parametric T1 maps were created automatically on the scanner and sent to our picture archiving and communication system (PACS IDS7, version 21.2, Sectra AB, Linköping, Sweden).

2.3. Image analysis

All images were analyzed by a trained doctoral student (D.C.; with 1 year of experience in liver MRI), and every case was visually controlled by two board-certified radiologists (V.C.O. and A.T.H. with 7 and 10 years of experience in liver MRI) who adapted contours when necessary. Sectra Workstation PACS IDS7 (version 21.2, Sectra AB, Linköping, Sweden) was used for image analyses. T1 relaxation times of the liver and spleen were measured by drawing a region of interest (ROI) covering each liver segment and the spleen (Fig. 2, A, B, D and E). An average value for the liver was then calculated from the individual

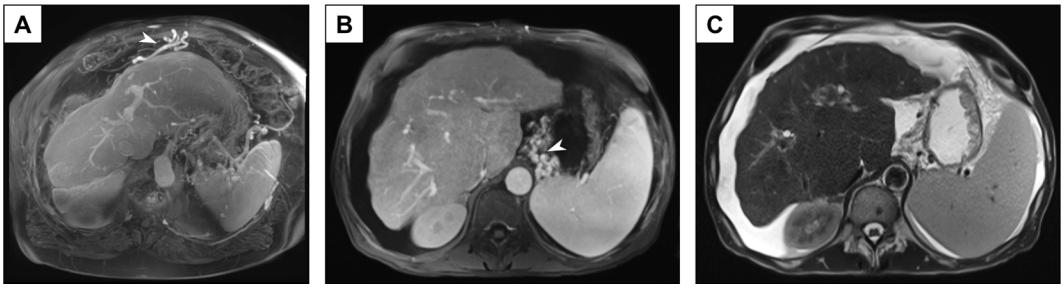

Fig. 3. Examples of observed signs of clinically significant portal hypertension. Fig. 3. Image A shows the recanalized umbilical vein (arrow) and splenomegaly in an 85-year-old male patient with alcoholic liver cirrhosis (Child C) and decompensated CSPH (dCSPH) visualized with a maximum intensity projection (MIP) reconstruction on a T1 VIBE fat-saturated sequence in the venous phase during a breath-hold examination. Image B is of a 66-year-old male patient with alcoholic liver cirrhosis (Child B) and decompensated CSPH (dCSPH) with gastroesophageal varices (B, arrow) and splenomegaly on a T1 VIBE fat-saturated sequence in the venous phase during a breath-hold examination. Image C shows marked ascites of the same 66-year-old patient on a T2-weighted half-Fourier acquisition single-shot turbo spin echo (HASTE) sequence.

measurements in the liver. The ROIs were drawn to cover the largest possible area of liver parenchyma at the same position in pre- and postcontrast T1 maps without including large blood vessels and bile ducts. While placing the ROIs, a distance from the organ capsule of at least 1 cm was maintained. In addition to the liver parenchyma, the blood pool was measured in the abdominal aorta on the same T1 maps in the diastolic phase of the cardiac cycle using pulse triggering. ΔT1 of the liver and spleen and the ECV of the spleen were calculated as follows [6,20]:

$$\Delta T1\ liver = \frac{native\ T1\ liver - postcontrast\ T1\ liver}{native\ T1\ liver}$$

$$\Delta T1\ spleen = \frac{native\ T1\ spleen - postcontrast\ T1\ spleen}{native\ T1\ spleen}$$

$$ECV\ spleen = (1 - hematocrit) \times \frac{(1/postcontrast\ T1\ spleen) - (1/native\ T1\ spleen)}{(1/postcontrast\ T1\ aorta) - (1/native\ T1\ aorta)}$$

In addition, the largest diameter of the spleen was measured in the longest axial direction on T2-weighted images (Fig. 2, C and F). The presence or absence of ascites and portosystemic collaterals, such as a recanalized paraumbilical vein, gastroesophageal varices and splenorenal collaterals, was determined on T2-weighted images with a 6-mm slice thickness and T1 VIBE fat-saturated contrast-enhanced images in the venous phase with a 3-mm slice thickness (Fig. 3).

2.4. Patient groups

Clinical data within a period of three months of the MR examination and information on the indication for the MR examination were collected from our clinical information system. For patients with liver cirrhosis, the Child-Pugh score was calculated. Patients were assigned to groups based on the presence or absence of clinically significant portal hypertension (CSPH) as defined in the Baveno VI consensus statement [22]. CSPH was defined as the presence of at least one of the following surrogate findings: 1) splenomegaly on MRI (>12 cm measured in the largest diameter) with concurrent thrombocytopenia ($<100 \times 10^9$ thrombocytes/L blood); 2) ascites on MRI; and 3) portosystemic collaterals on MRI. Patients without any of these surrogate findings were classified as having noCSPH. Patients with CSPH without ascites were allocated to the compensated CSPH subgroup (cCSPH), and CSPH patients with ascites were assigned to the decompensated CSPH subgroup (dCSPH).

2.5. Statistical analyses

All statistical analyses were performed using GraphPad Prism (version 9.0.1., GraphPad Software, San Diego, California, USA) and IBM SPSS Statistics (version 25.0, IBM Corporation, Armonk, New York, USA). The Shapiro-Wilk test that was performed to assess the parameters for normal distribution in the groups found that the values were not normally distributed; therefore, nonparametric tests were used for all analyses. Parameters among noCSPH, cCSPH and dCSPH were compared using the Kruskal-Wallis test with Dunn's multiple comparison post hoc test for continuous variables or the χ^2-test with a post hoc test consisting of a Z-test with Bonferroni correction for categorical variables [23]. Possible differences in ΔT1 of the liver, ΔT1 of the spleen and ECV of the spleen between the 1.5T and 3T groups were compared with a Mann-Whitney U test for all patient groups. Receiver operating characteristic (ROC) curve analyses were performed for single parameters (ΔT1 liver, ΔT1 spleen and ECV spleen). Cutoff values were determined using Youden's index. A multivariate logistic regression analysis was performed for combined parameters (ΔT1 liver + ΔT1 spleen; ΔT1 liver + ECV spleen) with CSPH as the outcome, and the results were used to calculate combined-parameter ROC curves for comparison with the single-parameter ROC curves. A p-value of 0.05 or less was defined as statistically significant.

3. Results

3.1. Indications for MR examination

The most frequent indication for MR examination in our study population was the evaluation of liver lesions (n = 85) followed by follow-up examinations in patients with HCC (n = 49) and HCC screening in patients with chronic liver disease (n = 18). Moreover, 13 examinations were performed as follow-up examinations in patients with liver metastases, and 6 examinations were performed for the evaluation of neuroendocrine tumors. Furthermore, 5 examinations were performed to evaluate pancreatic lesions, and 19 examinations were performed for other reasons.

Table 1
Patient characteristics.

Parameter	noCSPH *(n = 113)*	cCSPH *(n = 55)*	dCSPH *(n = 27)*	p-value
Male, n (%)	65 (58%)	35 (64%)	23 (85%)^{Z}	0.028
Age, years	65 (53–73)	62 (56–67)	68 (63–72) **	0.035
BMI, kg/m^2	26 (23–29)	28 (25–31)*	28 (23–30)	0.035
Arterial hypertension, n (%)	55 (49%)	27 (49%)	13 (48%)	0.997
Therapy for portal hypertension with nonselective β-blocker, n (%)	0 (0%)	24 (44%)^{Z}	14 (52%)^{Z}	<0.001
Daily alcohol consumption, n (%)	13 (12%)	11 (20%)	12 (44%)^{Z}	<0.001
Diabetes mellitus, n (%)	27 (24%)	18 (33%)	9 (33%)	0.379
Chronic liver disease, n (%)	65 (58%)	55 (100%)^{Z}	27 (100%)^{Z}	<0.001
CLD without cirrhosis, n	46	0	0	
Child A, n	16	38	3	
Child B, n	3	15	16	
Child C, n	0	2	8	
Signs of clinically significant portal hypertension, n (%)	0 (0%)	55 (100%)^{Z}	27 (100%)^{Z}	<0.001
Splenomegaly with concurrent thrombocytopenia, n	0	22	8	
Collaterals, n	0	55	22	
Ascites, n	0	0	27	
Creatinine, µmol/l	72 (63–85)	74 (58–86)	89 (62–135) *	0.045
Albumin, g/L	37 (34–40)	35 (32–38)	30 (22–35) */**	<0.001
Bilirubin, µmol/l	9 (6–14)	15 (10–22)*	17 (13–38)*	<0.001
AST, U/l	33 (23–53)	42 (34–69)*	46 (35–67)*	<0.001
ALT, U/l	33 (22–57)	33 (24–50)	29 (23–48)	0.723
Alkaline phosphatase, U/l	78 (66–104)	99 (75–130)	144 (109–224) */**	<0.001
GGT, U/l	50 (26–129)	108 (50–217)*	241 (98–387)*	<0.001
Hematocrit, %	40 (36–43)	39 (35–42)	32 (28–39) */**	<0.001
Thrombocytes, G/L	226 (183–279)	106 (72–135)*	125 (85–176)*	<0.001
Quick, %	94 (82–104)	77 (65–88)*	61 (51–78)*	<0.001
FIB-4	1.6 (1.0–2.4)	5.3 (2.7–7.5)*	5.6 (3.8–9.5)*	<0.001
APRI	0.35 (0.21–0.66)	1.27 (0.67–2.10) *	1.01 (0.63–2.12) *	<0.001

Values are presented as median with interquartile range (25–75%) or n (%). P-values were calculated using the Kruskal-Wallis test with Dunn's multiple comparison post hoc test or χ^2-test as appropriate. * = $p < 0.05$ in Dunn's multiple comparison test with noCSPH; ** = $p < 0.05$ in Dunn's multiple comparison test with cCSPH. ^{Z} = $p < 0.05$ in post hoc Z-tests with Bonferroni-adjusted p-value with noCSPH. Daily alcohol consumption was defined as ≥ 2 alcoholic beverages per day for men and ≥ 1 alcoholic beverage per day for women or the presence of a history of abusive alcohol consumption. Please note that patients could have multiple signs of portal hypertension at the same time. BMI = Body mass index; CLD = Chronic liver disease; AST = Aspartate aminotransferase; ALT = Alanine aminotransferase; GGT = Gamma-glutamyl-transferase; FIB-4 = Fibrosis-4 index; APRI = Aspartate aminotransferase to platelet ratio index; noCSPH = No clinically significant portal hypertension; cCSPH = Compensated clinically significant portal hypertension; dCSPH = Decompensated clinically significant portal hypertension.

Table 2
Results for the liver.

Parameter	noCSPH	cCSPH	dCSPH	p-value
1.5T	*(n = 61)*	*(n = 26)*	*(n = 13)*	
Native T1 liver, ms	590 (546–651)	668 (634–740) *	718 (673–903) *	<0.001
ΔT1 liver	0.70 (0.62–0.75)	0.61 (0.57–0.67)*	0.57 (0.45–0.68)*	<0.001
3T	*(n = 52)*	*(n = 29)*	*(n = 14)*	
Native T1 liver, ms	875 (815–937)	1001 (926–1058)*	991 (891–1091)*	<0.001
ΔT1 liver	0.74 (0.67–0.79)	0.65 (0.53–0.69)*	0.54 (0.44–0.57)*	<0.001
1.5T + 3T pooled	*(n = 113)*	*(n = 55)*	*(n = 27)*	
ΔT1 liver	0.71 (0.65–0.77)	0.62 (0.56–0.69)*	0.54 (0.46–0.63)*	<0.001

Values are presented as median with interquartile range (25–75%). P-values were calculated using the Kruskal-Wallis test with Dunn's multiple comparison post hoc test. * = $p < 0.05$ on Dunn's multiple comparison test with noCSPH. noCSPH = No clinically significant portal hypertension; cCSPH = Compensated clinically significant portal hypertension; dCSPH = Decompensated clinically significant portal hypertension.

Table 3
Results for the spleen.

Parameter	noCSPH	cCSPH	dCSPH	p-value
1.5T	*(n = 61)*	*(n = 26)*	*(n = 13)*	
Native T1 spleen, ms	1094 (1055–1154)	1137 (1113–1222)*	1181 (1144–1303)*	<0.001
ΔT1 spleen	0.31 (0.25–0.35)	0.34 (0.31–0.40)*	0.38 (0.32–0.42)*	0.005
ECV spleen	39.9 (34.5–46.2)	47.4 (36.9–49.8)	48.9 (42.3–57.1)*	0.009
3T	*(n = 52)*	*(n = 29)*	*(n = 14)*	
Native T1 spleen, ms	1346 (1230–1425)	1383 (1254–1500)	1345 (1256–1577)	0.226
ΔT1 spleen	0.29 (0.25–0.34)	0.32 (0.28–0.38)	0.35 (0.30–0.39)*	0.006
ECV spleen	44.6 (36.3–51.3)	44.7 (40.8–55.0)	49.2 (41.8–59.5)	0.207
1.5T + 3T pooled	*(n = 113)*	*(n = 55)*	*(n = 27)*	
ΔT1 spleen	0.29 (0.25–0.35)	0.34 (0.30–0.39)*	0.35 (0.32–0.42)*	<0.001
ECV spleen	41.3 (35.8–50.1)	46.6 (39.7–50.3)	48.9 (42.1–59.4)*	0.002

Values are presented as median with interquartile range (25–75%). P-values were calculated using the Kruskal-Wallis test with Dunn's multiple comparison post hoc test. * = $p < 0.05$ on Dunn's multiple comparison test with noCSPH. noCSPH = No clinically significant portal hypertension; cCSPH = Compensated clinically significant portal hypertension; dCSPH = Decompensated clinically significant portal hypertension; ECV = Extracellular volume fraction.

3.2. Patient characteristics

The patient characteristics are shown in Table 1. Of the 195 patients, 113 patients had noCSPH (61 at 1.5T and 52 at 3T), 55 patients had cCSPH (26 at 1.5T and 29 at 3T) and 27 patients had dCSPH (13 at 1.5T and 14 at 3T). Patients in the CSPH group had more cases of diabetes, higher daily alcohol consumption and higher average body mass index (BMI) than patients in the noCSPH group. FIB-4 and APRI were higher in CSPH than in noCSPH, which agreed with the clinical patient data. In the noCSPH group, only 58% of patients had CLD, whereas in the CSPH group, all patients were affected by CLD. The most common etiologies

Table 4
ROC curve analysis.

Parameter	Cutoff value	AUC	Sensitivity, %	Specificity, %	NPV, %	PPV, %	Youden's index	p-value
noCSPH vs. CSPH								
ΔT1 liver	< 0.67	0.79	74	72	79	66	46	<0.001
ΔT1 spleen	> 0.29	0.69	80	51	78	54	31	<0.001
ECV spleen	> 41.9	0.63	72	54	73	53	26	0.001
noCSPH vs. cCSPH								
ΔT1 liver	< 0.67	0.75	69	72	83	55	41	<0.001
ΔT1 spleen	> 0.28	0.67	84	44	85	42	28	<0.001
ECV spleen	> 41.5	0.60	71	52	79	42	23	0.032
noCSPH vs. dCSPH								
ΔT1 liver	< 0.64	0.87	81	78	95	47	59	<0.001
ΔT1 spleen	> 0.29	0.74	89	51	95	30	40	<0.001
ECV spleen	> 40.8	0.70	89	48	95	29	37	0.001

ROC = Receiver operating characteristic; AUC = Area under the curve; NPV = Negative predictive value; PPV = Positive predictive value; noCSPH = No clinically significant portal hypertension; CSPH = Clinically significant portal hypertension; cCSPH = Compensated clinically significant portal hypertension; dCSPH = Decompensated clinically significant portal hypertension; ECV = Extracellular volume fraction. Number of patients in each group: noCSPH (n = 113), CSPH (n = 82), cCSPH (n = 55) and dCSPH (n = 27).

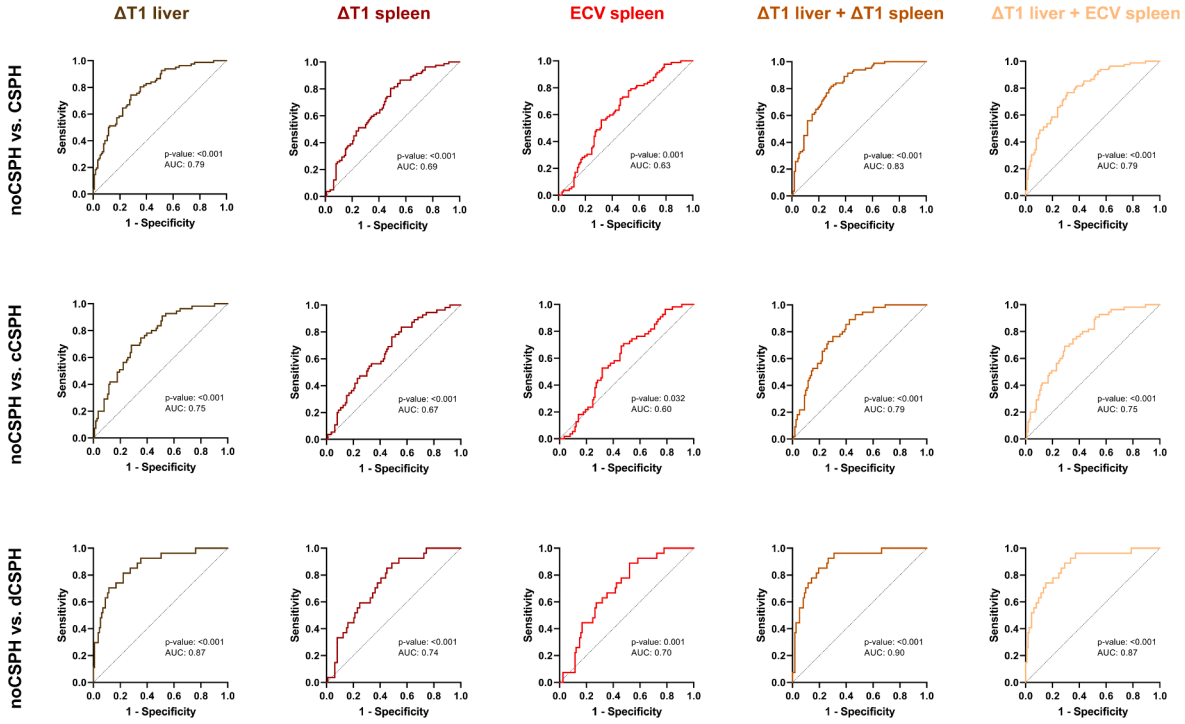

Fig. 4. ROC curves. Fig. 4. Fig. 4 shows the ROC curves for noCSPH vs. CSPH, noCSPH vs. cCSPH and noCSPH vs. dCSPH for ΔT1 of the liver, ΔT1 of the spleen, ECV of the spleen, a combination of ΔT1 of the liver + ΔT1 of the spleen and a combination of ΔT1 of the liver + ECV of the spleen. The p-value and the area under the curve (AUC) are given for each ROC curve. noCSPH = No clinically significant portal hypertension; cCSPH = Compensated clinically significant portal hypertension; dCSPH = Decompensated clinically significant portal hypertension; ECV = Extracellular volume fraction; AUC = Area under the curve.

for CLD were NAFLD/NASH (21 in the noCSPH group and 12 in the CSPH group), ARLD/ASH (13 in the noCSPH group and 27 in the CSPH group), chronic viral hepatitis (14 in the noCSPH group and 12 in the CSPH group) and PSC/PBC (6 in the noCSPH group and 4 in the CSPH group). Fourteen patients with noCSPH and 6 patients with CSPH had other etiologies.

3.3. Results for the liver

The native T1 relaxation times of the liver were significantly longer in patients with cCSPH and dCSPH than in patients with noCSPH both at 1.5TT (noCSPH 590 ms, cCSPH 668 ms, $p < 0.001$; dCSPH 718 ms, $p < 0.001$) and at 3T (noCSPH 875 ms, cCSPH 1001 ms, $p < 0.001$; dCSPH 991 ms, $p = 0.011$). Furthermore, ΔT1 of the liver was significantly lower in patients with cCSPH and dCSPH than in patients with noCSPH at 1.5T (noCSPH 0.70, cCSPH 0.61, $p = 0.002$; dCSPH 0.57, $p = 0.003$), 3T (noCSPH 0.74, cCSPH 0.65, $p < 0.001$; dCSPH 0.54, $p < 0.001$) and in the pooled analysis (noCSPH 0.71, cCSPH 0.62, $p < 0.001$; dCSPH 0.54, $p < 0.001$). Even if there was a tendency of a lower ΔT1 of the liver in patients with dCSPH compared to patients with cCSPH, statistical significance was not reached ($p > 0.999$ at 1.5T; $p = 0.081$ at 3T; and $p = 0.088$ in pooled analysis) (Table 2).

3.4. Results for the spleen

The native T1 relaxation times of the spleen were significantly longer

Table 5
Combined ROC curve analysis.

Parameter	AUC	Sensitivity, %	Specificity, %	NPV, %	PPV, %	p-value
noCSPH vs. CSPH						
ΔT1 liver (<0.67) + ΔT1 spleen (>0.29)	0.83	61	83	75	72	<0.001
ΔT1 liver (<0.67) + ECV spleen (>41.9)	0.79	54	88	73	77	<0.001
noCSPH vs. cCSPH						
ΔT1 liver (<0.67) + ΔT1 spleen (>0.28)	0.79	56	82	79	61	<0.001
ΔT1 liver (<0.67) + ECV spleen (>41.5)	0.75	49	88	78	66	<0.001
noCSPH vs. dCSPH						
ΔT1 liver (<0.64) + ΔT1 spleen (>0.29)	0.90	70	88	93	58	<0.001
ΔT1 liver (<0.64) + ECV spleen (>40.8)	0.87	74	91	94	67	<0.001

Values were calculated based on a logistic regression analysis with a classification cutoff of 0.5.
ROC = Receiver operating characteristic; AUC = Area under the curve; NPV = Negative predictive value; PPV = Positive predictive value; noCSPH = No clinically significant portal hypertension; CSPH = Clinically significant portal hypertension; cCSPH = Compensated clinically significant portal hypertension; dCSPH = Decompensated clinically significant portal hypertension; ECV = Extracellular volume fraction. Number of patients in each group: noCSPH (n = 113), CSPH (n = 82), cCSPH (n = 55) and dCSPH (n = 27).

in patients with cCSPH and dCSPH than in patients with noCSPH at 1.5T (noCSPH 1094 ms, cCSPH 1137 ms, p = 0.027; dCSPH 1181 ms, p = 0.003) but not at 3T (noCSPH 1346 ms, cCSPH 1383 ms, p = 0.423; dCSPH 1345 ms, p = 0.614). Furthermore, pooled ΔT1 of the spleen was significantly higher in patients with cCSPH and dCSPH than in patients with noCSPH (noCSPH 0.29, cCSPH 0.34, p = 0.003; dCSPH 0.35, p < 0.001). In the pooled analysis, the ECV of the spleen was significantly higher in patients with dCSPH than in patients with noCSPH (noCSPH 41.3, dCSPH 48.9, p = 0.003) but not in patients with cCSPH (46.6, p = 0.112). There was no significant difference in the pooled analysis between cCSPH and dCSPH for ΔT1 of the spleen (cCSPH 0.34, dCSPH 0.35, p = 0.688) and the ECV of the spleen (cCSPH 46.6, dCSPH 48.9, p = 0.35) (Table 3).

3.5. Comparison between 1.5T and 3T

In patients with noCSPH, ΔT1 of the liver was 0.70 (0.62–0.75) at 1.5T and 0.74 (0.67–0.79) at 3T (p = 0.055). In patients with cCSPH, ΔT1 of the liver was 0.61 (0.57–0.67) at 1.5T and 0.65 (0.53–0.69) at 3T (p = 0.622). In patients with dCSPH, ΔT1 of the liver was 0.57 (0.45–0.68) at 1.5T and 0.54 (0.44–0.57) at 3T (p = 0.302).

In patients with noCSPH, ΔT1 of the spleen was 0.31 (0.25–0.35) at 1.5T and 0.29 (0.25–0.34) at 3T (p = 0.360), while the ECV of the spleen was 39.9 (34.5–46.2) at 1.5T and 44.6 (36.3–51.3) at 3T (p = 0.073). In patients with cCSPH, ΔT1 of the spleen was 0.34 (0.31–0.40) at 1.5T and 0.32 (0.28–0.38) at 3T (p = 0.407), while the ECV of the spleen was 47.4 (36.9–49.8) at 1.5T and 44.7 (40.8–55.0) at 3T (p = 0.466). In patients with dCSPH, ΔT1 of the spleen was 0.38 (0.32–0.42) at 1.5T and 0.35 (0.30–0.39) at 3T (p = 0.488), while the ECV of the spleen was 48.9 (42.3–57.1) at 1.5T and 49.2 (41.8–59.5) at 3T (p = 0.867).

3.6. Results of the ROC curve analyses

All ROC curve analyses showed significant results. With regard to a cutoff value to distinguish between noCSPH and CSPH patients, the best performance was observed for ΔT1 of the liver with a cutoff value of < 0.67, which predicted CSPH with a negative predictive value (NPV) of 79% and a positive predictive value (PPV) of 66% (AUC = 0.79). ΔT1 of the liver was also the best parameter for distinguishing between noCSPH and cCSPH with a NPV of 83% and a PPV of 55% (AUC = 0.75) when using a cutoff value of < 0.67. An even higher performance of ΔT1 of the liver was observed when differentiating between noCSPH and dCSPH with a NPV of 95% and a PPV of 47% (AUC = 0.87) when using a cutoff value of < 0.64 (Table 4).

When cutoff values for ΔT1 of the liver, ΔT1 of the spleen and ECV of the spleen were combined, the AUC was larger (Fig. 4) with a higher positive predictive value for CSPH (PPV = 72% for combination of ΔT1 of the liver < 0.67 and ΔT1 of the spleen > 0.29; PPV = 77% for combination of ΔT1 of the liver < 0.67 and the ECV of the spleen > 41.9), cCSPH (PPV = 61% for combination of ΔT1 of the liver < 0.67 and ΔT1 of the spleen > 0.28; PPV = 66% for combination of ΔT1 of the liver < 0.67 and the ECV of the spleen > 41.5) and dCSPH (PPV = 58% for combination ΔT1 of the liver < 0.64 and ΔT1 of the spleen > 0.29; PPV = 67% for combination of ΔT1 of the liver < 0.64 and the ECV of the spleen > 40.8) (Table 5). The odds ratios of the multiple logistic regression analysis are shown in Appendix B.

4. Discussion

This is the first study to show that ΔT1 of the liver, ΔT1 of the spleen and ECV of the spleen allow for the determination of CSPH using routine Gd-EOB-DTPA liver MRI. The best overall performance was achieved by combining ΔT1 of the liver and ΔT1 of the spleen, while the highest positive predictive value was achieved by combining ΔT1 of the liver and the ECV of the spleen. Therefore, multiparametric T1 mapping of the liver and spleen is a reliable method to determine the presence of clinically significant portal hypertension using routine Gd-EOB-DTPA liver MRI. Because T1 mapping sequences are available on any scanner without the need for additional hardware, they are more widely available than MRE. With an additional acquisition time of no>4 min, clinicians may depict patients with CLD and portal hypertension earlier using routine Gd-EOB-DTPA liver MRI in the future, allowing better risk stratification and earlier initiation of treatment for the prevention of complications.

In the liver, there was a tendency for a lower ΔT1 in patients with dCSPH than in patients with cCSPH, but statistical significance was not reached. Of note, the ECV of the liver could not be evaluated due to the use of Gd-EOB-DTPA. The present study did not investigate whether a lower ΔT1 of the liver might be explained by a decrease in hepatocellular function in decompensated patients, thereby further studies that include more patients with dCSPH are warranted. In the spleen, there was no significant difference between ΔT1 and ECV between cCSPH

patients and dCSPH patients. We hypothesized that a lower ΔT1 of the liver reflects decreased hepatocellular function, which is directly linked to the occurrence of compensated and decompensated CSPH. In addition, we also hypothesized that a higher ΔT1 and ECV of the spleen directly measure the extension of the splenic extracellular space due to CSPH, which is unrelated to whether the patents are compensated or decompensated. However, these hypotheses should be investigated in future studies.

Our results agreed with recent publications. ΔT1 of the liver is known to be significantly reduced in patients with CLD, and it correlates with liver function on Gd-EOB-DTPA liver MRI [24,25]. Ding et al. showed that ΔT1 of the liver is lower in patients with significant liver fibrosis (mean ΔT1 = 0.66 for fibrosis grade 3–4) than in patients without significant liver fibrosis (mean ΔT1 = 0.71 for fibrosis grade 0–2) at 1.5T [26]. The values in patients without significant liver fibrosis from the study of Ding et al. are comparable to the ΔT1 values observed in noCSPH patients in our study. In cCSPH and dCSPH patients, ΔT1 was lower, thus reflecting the decreased function of hepatocytes in these patients.

Studies analyzing T1 mapping of the spleen are sparse. A recent publication has shown a longer T1 relaxation time of the spleen at 3T in patients with significantly elevated liver stiffness on MR elastography [27], which was in accordance with the present study. Another study has shown increased ECV of the spleen in patients with end-stage liver cirrhosis and severe portal hypertension undergoing a TIPS procedure [6], which agreed with our study, showing a significantly higher ECV of the spleen in CSPH patients than in noCSPH patients. However, the absolute ECV values of the spleen were slightly lower in the study by Mesropyan et al. in both groups, which may be related to differences between the sequences used and MR scanners from different vendors as well as different contrast agents. Mesropyan et al. used gadobutrol, which is an extracellular contrast agent, while Gd-EOB-DTPA, which was used in the present study, is a hepatocyte-specific contrast agent with only one part of the administered Gd-EOB-DTPA distributed to the extracellular space of the spleen. In addition, gadobutrol has a different relaxivity than Gd-EOB-DTPA [28], and the timing to measure the ECV of the spleen differed between the two studies (10 min after gadobutrol injection vs. 20 min after Gd-EOB-DTPA injection). Even if gadobutrol is more suitable for ECV calculation in the spleen, Gd-EOB-DTPA is more widely used for liver MRI in routine clinical practice. Finally, the use of gadobutrol allows the calculation of splenic ECV but not in combination with ΔT1 of the liver to determine liver function.

Apart from MRI T1 mapping, there have been other noninvasive MRI techniques to assess portal hypertension [29]. For instance, liver stiffness values measured by MRE correlate significantly with the hepatic venous pressure gradient (HVPG) and allow for the detection of patients with clinically significant portal hypertension with an AUROC of 0.74, a sensitivity of 55% and a specificity of 91% [30]. Interestingly, this performance was similar to the combined prediction of ΔT1 and ECV of the liver and spleen in the present study. MRE measures the increased tissue stiffness of the liver and spleen due to liver fibrosis and CSPH, while ΔT1 and ECV measure the expansion of the extracellular space of the spleen due to CSPH. Therefore, it might be interesting to combine ΔT1 and ECV of the liver and spleen with MRE in an upcoming study to analyze whether a combination of both methods may incrementally increase the predictive value to determine CSPH. Computed tomography studies have used the liver surface nodularity (LSN) score to detect patients with clinically significant portal hypertension [31]. LSN has been successfully applied to liver MRI to detect advanced liver fibrosis [32], and it has also been shown to correlate with the degree of portal hypertension [12]. It would therefore be interesting to combine ΔT1 of the liver, ΔT1 of the and spleen and ECV of the spleen with MRE and the MRI-derived LSN score to determine the presence and severity of CSPH in patients undergoing routine Gd-EOB-DTPA liver MRI.

The present study had several limitations. First, this was a retrospective study with a heterogeneous patient population. However, due to stringent inclusion and exclusion criteria, major confounding factors were minimized, and the study population was well characterized. Another potential limitation was that our study was conducted using both 1.5T and 3T scanners. Due to the measurement of a ratio with relative T1 shortening of the spleen, however, there should not be a large difference between different field strengths as this has been shown for the ECV in other tissue types, such as the myocardium, and for ΔT1 of the liver with similar values at 1.5T and 3T [33]. A subanalysis in our patient population showed no significant difference between the different field strengths. Nevertheless, the results of the present study should be validated in further prospective studies. Finally, there were no invasive measurements of the hepatic venous pressure gradient, which was not possible due to ethical considerations in this patient population. However, the presented clinical approach to determine CSPH allowed us to investigate a large cross-sectional study in a realistic setting of patients in a radiology department undergoing liver MRI with Gd-EOB-DTPA.

5. Conclusions

In conclusion, ΔT1 of the liver, ΔT1 of the and spleen and ECV of the spleen allow for the determination of CSPH using routine Gd-EOB-DTPA liver MRI in a clinical setting. Consequently, ΔT1 of the liver and spleen as well as the ECV of the spleen may be helpful imaging biomarkers to characterize patients with CLD more accurately to allow both improved risk stratification and better individualized therapy of CSPH without relying on invasive portal venous pressure measurement.

When using ΔT1 of the liver, ΔT1 of the and spleen and ECV of the spleen to detect CSPH, a combination of both decreased ΔT1 of the liver and increased ΔT1 and ECV of the spleen may perform better than ΔT1 of the liver alone as this combination showed a notably higher positive predictive value for CSPH in our study. However, whether this combination of parameters is also associated with adverse outcomes warrants further investigation.

- D.C., A.T.H., study concepts/study design
- D.C., A.T.H., V.C.O., data acquisition or data analysis/interpretation
- All authors: manuscript drafting or manuscript revision for important intellectual content
- All authors: approval of final version of submitted manuscript
- All authors: literature research

Funding

This project was funded by the Swiss National Science Foundation (SNSF), grant number #188591.

Declaration of Competing Interest

The authors declare that they have no known competing financial interests or personal relationships that could have appeared to influence the work reported in this paper.

Acknowledgements

The authors thank the MR imaging technicians and the imaging core lab team from the Department of Diagnostic, Interventional and Pediatric Radiology at the University Hospital of Bern for their support, especially Michelle Schweizer, Géraldine Gemmet, Franziska Theiler, Sylvia Büttiker and Albert Muhaxheri.

Appendix A

See Table A1.

Table A1
Specifications of MRI sequences.

Sequence	Plane	TR, ms	TE, ms	Flip angle	Fat saturation	Slice thickness, mm
HASTE	axial	1,400	95	160°	No	5
HASTE	coronal	1,200	92	175°	Yes	5
T1 VIBE	axial	4.49	2.19	10°	Yes	3
DWI	axial	7,300	54	90°	No	5
T1 maps	axial	281	1.12	35°	No	8

In appendix A, the specifications of the MRI sequences used are shown. The used b-values for diffusion-weighted imaging were b = 0, b = 400 and b = 800 s/mm^2. MR = Magnetic resonance; HASTE = Half-Fourier acquisition single-shot turbo spin echo; VIBE = Volumetric interpolated breath-hold examination; TR = Time to repeat; TE = Time to echo; DWI = Diffusion-weighted imaging.

Appendix B

See Table B1.

Table B1
Odds ratios of multiple logistic regression.

	Parameter	Odds ratio	Lower 95% CI-level	Upper 95% CI-level	p-value
noCSPH vs. CSPH	**ΔT1 liver (<0.67) + ΔT1 spleen (>0.29)**				
	ΔT1 liver	0.90	0.86	0.93	<0.001
	ΔT1 spleen	1.09	1.04	1.14	<0.001
	ΔT1 liver (<0.67) + ECV spleen (>41.9)				
	ΔT1 liver	0.90	0.86	0.93	<0.001
	ECV spleen	1.00	0.99	1.03	0.498
noCSPH vs. cCSPH	**ΔT1 liver (<0.67) + ΔT1 spleen (>0.28)**				
	ΔT1 liver	0.91	0.87	0.94	<0.001
	ΔT1 spleen	1.07	1.02	1.13	0.009
	ΔT1 liver (<0.67) + ECV spleen (>41.5)				
	ΔT1 liver	0.91	0.87	0.94	<0.001
	ECV spleen	1.00	0.98	1.03	0.779
noCSPH vs. dCSPH	**ΔT1 liver (<0.64) + ΔT1 spleen (>0.29)**				
	ΔT1 liver	0.88	0.83	0.92	<0.001
	ΔT1 spleen	1.09	1.02	1.17	0.019
	ΔT1 liver (<0.64) + ECV spleen (>40.8)				
	ΔT1 liver	0.88	0.82	0.92	<0.001
	ECV spleen	1.02	0.99	1.05	0.161

In appendix B, the odds ratios of the multiple logistic regression are shown.
CI = Confidence interval; noCSPH = No clinically significant portal hypertension; CSPH = Clinically significant portal hypertension; cCSPH = Compensated clinically significant portal hypertension; dCSPH = Decompensated clinically significant portal hypertension; ECV = Extracellular volume fraction. Number of patients in each group: noCSPH (n = 113), CSPH (n = 82), cCSPH (n = 55) and dCSPH (n = 27).

References

[1] L. Turco, G. Garcia-Tsao, Portal Hypertension: Pathogenesis and Diagnosis, Clin. Liver Dis. 23 (4) (2019) 573–587, https://doi.org/10.1016/j.cld.2019.07.007.

[2] X. Qi, A. Berzigotti, A. Cardenas, S.K. Sarin, Emerging non-invasive approaches for diagnosis and monitoring of portal hypertension, The Lancet, Gastroenterol. Hepatol. 3 (10) (2018) 708–719, https://doi.org/10.1016/S2468-1253(18)30232-2.

[3] Y.-W. Zheng, K.-P. Wang, J.-J. Zhou, Z.-Q. Zhang, L.i. Xiong, Y.u. Wen, H. Zou, Portal hypertension predicts short-term and long-term outcomes after hepatectomy in hepatocellular carcinoma patients, Null. 53 (12) (2018) 1562–1568, https://doi.org/10.1080/00365521.2018.1538386.

[4] A. Berzigotti, M. Reig, J.G. Abraldes, J. Bosch, J. Bruix, Portal hypertension and the outcome of surgery for hepatocellular carcinoma in compensated cirrhosis: A systematic review and meta-analysis, Hepatology 61 (2) (2015) 526–536, https://doi.org/10.1002/hep.27431.

[5] J.W. Choi, J.W. Chung, D.H. Lee, H.-C. Kim, S. Hur, M. Lee, H.J. Jae, Portal hypertension is associated with poor outcome of transarterial chemoembolization in patients with hepatocellular carcinoma, Eur. Radiol. 28 (5) (2018) 2184–2193, https://doi.org/10.1007/s00330-017-5145-9.

[6] N. Mesropyan, A. Isaak, A. Faron, M. Praktiknjo, C. Jansen, D. Kuetting, C. Meyer, C.C. Pieper, A.M. Sprinkart, J. Chang, B. Maedler, D. Thomas, P. Kupczyk, U. Attenberger, J.A. Luetkens, Magnetic resonance parametric mapping of the spleen for non-invasive assessment of portal hypertension, Eur. Radiol. 31 (1) (2021) 85–93, https://doi.org/10.1007/s00330-020-07080-5.

[7] L. Pimpin, H. Cortez-Pinto, F. Negro, E. Corbould, J.V. Lazarus, L. Webber, N. Sheron, Burden of liver disease in Europe: Epidemiology and analysis of risk factors to identify prevention policies, J. Hepatol. 69 (3) (2018) 718–735, https://doi.org/10.1016/j.jhep.2018.05.011.

[8] E.A. Tsochatzis, J. Bosch, A.K. Burroughs, Liver cirrhosis, The Lancet. 383 (9930) (2014) 1749–1761, https://doi.org/10.1016/S0140-6736(14)60121-5.

[9] V.L. Mura, A. Nicolini, G. Tosetti, M. Primignani, Cirrhosis and portal hypertension: The importance of risk stratification, the role of hepatic venous pressure gradient measurement, World, J. Hepatol. 7 (2015) 688–695, https://doi.org/10.4254/wjh.v7.i4.688.

[10] V.C. Obmann, C. Marx, J. Hrycyk, A. Berzigotti, L. Ebner, N. Mertineit, C.h. Gräni, J.T. Heverhagen, A. Christe, A.T. Huber, Liver segmental volume and attenuation ratio (LSVAR) on portal venous CT scans improves the detection of clinically significant liver fibrosis compared to liver segmental volume ratio (LSVR), Abdom. Radiol. 46 (5) (2021) 1912–1921, https://doi.org/10.1007/s00261-020-02834-7.
[11] A. Huber, L. Ebner, M. Montani, N. Semmo, K. Roy Choudhury, J. Heverhagen, A. Christe, Computed tomography findings in liver fibrosis and cirrhosis, Swiss Medical Weekly. 144 (2014), https://doi.org/10.4414/smw.2014.13923.
[12] N. De Vos, R. Sartoris, F. Cauchy, P.-E. Rautou, V. Vilgrain, M. Ronot, Performance of liver surface nodularity quantification for the diagnosis of portal hypertension in patients with cirrhosis: comparison between MRI with hepatobiliary phase sequences and CT, Abdominal, Radiology 45 (2) (2020) 365–372, https://doi.org/10.1007/s00261-019-02355-y.
[13] J.R. Dillman, S.D. Serai, A.T. Trout, R. Singh, J.A. Tkach, A.E. Taylor, B.C. Blaxall, L. Fei, A.G. Miethke, Diagnostic performance of quantitative magnetic resonance imaging biomarkers for predicting portal hypertension in children and young adults with autoimmune liver disease, Pediatr. Radiol. 49 (3) (2019) 332–341, https://doi.org/10.1007/s00247-018-4319-1.
[14] C. Cassinotto, M. Feldis, J. Vergniol, A. Mouries, H. Cochet, B. Lapuyade, A. Hocquelet, E. Juanola, J. Foucher, F. Laurent, V. De Ledinghen, MR relaxometry in chronic liver diseases: Comparison of T1 mapping, T2 mapping, and diffusion-weighted imaging for assessing cirrhosis diagnosis and severity, Eur. J. Radiol. 84 (8) (2015) 1459–1465, https://doi.org/10.1016/j.ejrad.2015.05.019.
[15] V. Obmann, N. Mertineit, C. Marx, A. Berzigotti, L. Ebner, J.T. Heverhagen, A. Christe, A. Huber, Liver MR relaxometry at 3T – segmental normal T 1 and T 2 * values in patients without focal or diffuse liver disease and in patients with increased liver fat and elevated liver stiffness, Sci. Rep. 9 (2019) 8106, https://doi.org/10.1038/s41598-019-44377-y.
[16] T.K. Yasar, M. Wagner, O. Bane, C. Besa, J.S. Babb, S. Kannengiesser, M. Fung, R. L. Ehman, B. Taouli, Interplatform reproducibility of liver and spleen stiffness measured with MR elastography, J. Magnet. Resonance Imaging: JMRI. 43 (5) (2016) 1064–1072, https://doi.org/10.1002/jmri.25077.
[17] Y.-W. Cheng, Y.-C. Chang, Y.-L. Chen, R.-C. Chen, C.-T. Chou, H.-C. Lin, Feasibility of measuring spleen stiffness with MR elastography and splenic volume to predict hepatic fibrosis stage, PLoS ONE 14 (5) (2019) e0217876, https://doi.org/10.1371/journal.pone.0217876.
[18] H. Yoon, H.J. Shin, M.-J. Kim, S.J. Han, H. Koh, S. Kim, M.-J. Lee, Predicting gastroesophageal varices through spleen magnetic resonance elastography in pediatric liver fibrosis, World J. Gastroenterol. 25 (3) (2019) 367–377, https://doi.org/10.3748/wjg.v25.i3.367.
[19] S. Poetter-Lang, N. Bastati, A. Messner, A. Kristic, A. Herold, J.C. Hodge, A. Ba-Ssalamah, Quantification of liver function using gadoxetic acid-enhanced MRI, Abdom. Radiol. 45 (11) (2020) 3532–3544, https://doi.org/10.1007/s00261-020-02779-x.
[20] M. Haimerl, I. Fuhrmann, S. Poelsterl, C. Fellner, M.D. Nickel, K. Weigand, M. H. Dahlke, N. Verloh, C. Stroszczynski, P. Wiggermann, Gd-EOB-DTPA-enhanced T1 relaxometry for assessment of liver function determined by real-time 13C-methacetin breath test, Eur. Radiol. 28 (9) (2018) 3591–3600, https://doi.org/10.1007/s00330-018-5337-y.
[21] A.T. Huber, J. Lamy, M. Bravetti, K. Bouazizi, T. Bacoyannis, C. Roux, A. De Cesare, A. Rigolet, O. Benveniste, Y. Allenbach, M. Kerneis, P. Cluzel, A. Redheuil, N. Kachenoura, Comparison of MR T1 and T2 mapping parameters to characterize myocardial and skeletal muscle involvement in systemic idiopathic inflammatory myopathy (IIM), Eur. Radiol. 29 (10) (2019) 5139–5147, https://doi.org/10.1007/s00330-019-06054-6.
[22] R. de Franchis, Expanding consensus in portal hypertension: Report of the Baveno VI Consensus Workshop: Stratifying risk and individualizing care for portal hypertension, J. Hepatol. 63 (3) (2015) 743–752, https://doi.org/10.1016/j.jhep.2015.05.022.
[23] D. Sharpe, Chi-Square Test is Statistically Significant: Now What? Pract. Assess., Res., Eval. 20 (2015) https://doi.org/10.7275/tbfa-x148.
[24] T. Katsube, M. Okada, S. Kumano, M. Hori, I. Imaoka, K. Ishii, M. Kudo, H. Kitagaki, T. Murakami, Estimation of Liver Function Using T1 Mapping on Gd-EOB-DTPA-Enhanced Magnetic Resonance Imaging, Invest. Radiol. 46 (2011), https://doi.org/10.1097/RLI.0b013e318200f67d.
[25] J.H. Yoon, J.M. Lee, M. Paek, J.K. Han, B.I. Choi, Quantitative assessment of hepatic function: modified look-locker inversion recovery (MOLLI) sequence for T1 mapping on Gd-EOB-DTPA-enhanced liver MR imaging, Eur. Radiol. 26 (6) (2016) 1775–1782, https://doi.org/10.1007/s00330-015-3994-7.
[26] Y. Ding, S.-X. Rao, T. Zhu, C.-Z. Chen, R.-C. Li, M.-S. Zeng, Liver fibrosis staging using T1 mapping on gadoxetic acid-enhanced MRI compared with DW imaging, Clin. Radiol. 70 (10) (2015) 1096–1103, https://doi.org/10.1016/j.crad.2015.04.014.
[27] V.C. Obmann, A. Berzigotti, D. Catucci, L. Ebner, C. Gräni, J.T. Heverhagen, A. Christe, A.T. Huber, T1 mapping of the liver and the spleen in patients with liver fibrosis—does normalization to the blood pool increase the predictive value? Eur. Radiol. 31 (6) (2021) 4308–4318, https://doi.org/10.1007/s00330-020-07447-8.
[28] S. Aime, P. Caravan, Biodistribution of gadolinium-based contrast agents, including gadolinium deposition, J. Magn. Reson. Imaging 30 (6) (2009) 1259–1267, https://doi.org/10.1002/jmri.v30:610.1002/jmri.21969.
[29] A.M. Elmahdy, A. Berzigotti, Non-invasive Measurement of Portal Pressure, Curr. Hepatol.. Reports. 18 (1) (2019) 20–27, https://doi.org/10.1007/s11901-019-00446-4.
[30] M. Wagner, S. Hectors, O. Bane, S. Gordic, P. Kennedy, C. Besa, T.D. Schiano, S. Thung, A. Fischman, B. Taouli, Noninvasive prediction of portal pressure with MR elastography and DCE-MRI of the liver and spleen: Preliminary results, J. Magn. Reson. Imaging 48 (4) (2018) 1091–1103, https://doi.org/10.1002/jmri.26026.
[31] R. Sartoris, P.-E. Rautou, L. Elkrief, G. Pollorsi, F. Durand, D. Valla, L. Spahr, S. Terraz, O. Soubrane, F. Cauchy, V. Vilgrain, M. Ronot, Quantification of Liver Surface Nodularity at CT: Utility for Detection of Portal Hypertension, Radiology 289 (3) (2018) 698–707, https://doi.org/10.1148/radiol.2018181131.
[32] R. Catania, A. Furlan, A.D. Smith, J. Behari, M.E. Tublin, A.A. Borhani, Diagnostic value of MRI-derived liver surface nodularity score for the non-invasive quantification of hepatic fibrosis in non-alcoholic fatty liver disease, Eur. Radiol. 31 (1) (2021) 256–263, https://doi.org/10.1007/s00330-020-07114-y.
[33] N. Kawel-Boehm, S.J. Hetzel, B. Ambale-Venkatesh, G. Captur, C.J. Francois, M. Jerosch-Herold, M. Salerno, S.D. Teague, E. Valsangiacomo-Buechel, R.J. van der Geest, D.A. Bluemke, Reference ranges ("normal values") for cardiovascular magnetic resonance (CMR) in adults and children: 2020 update, J. Cardiovasc. Magn. Reson. 22 (2020) 87, https://doi.org/10.1186/s12968-020-00683-3.